

1

Supplementary Information

2

Discovering genetic interactions bridging pathways in genome-wide association studies

3

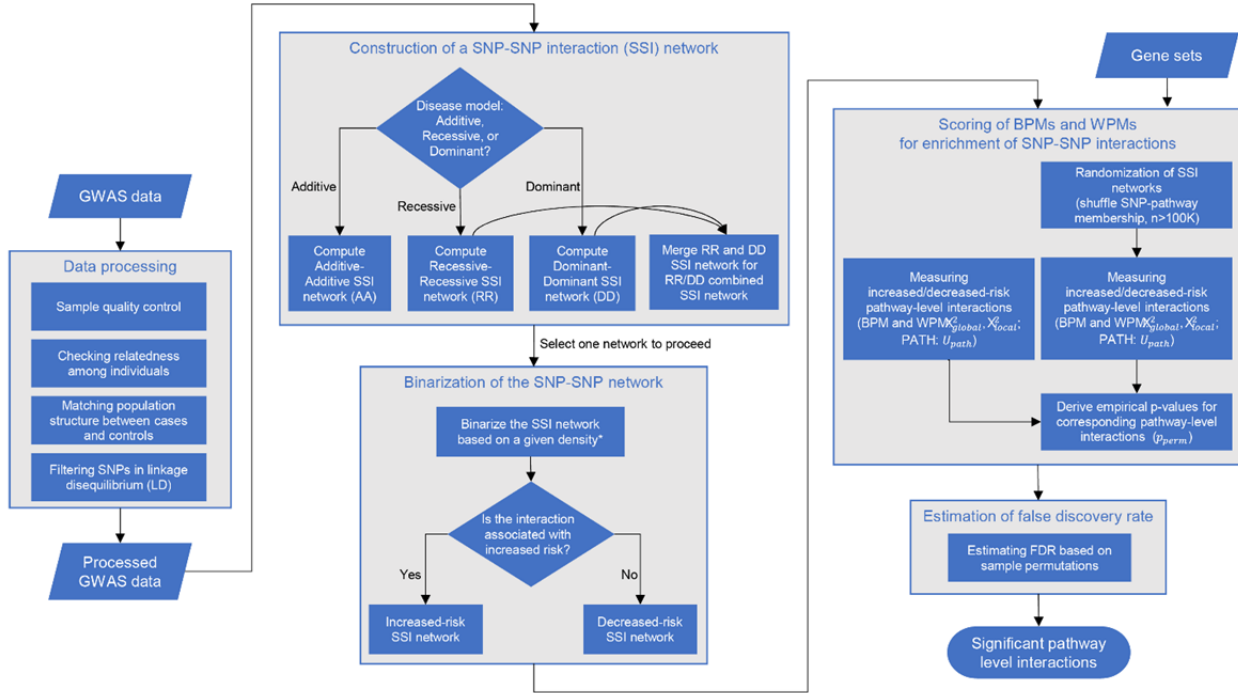
Fang and Wang et.al.

4

5

6

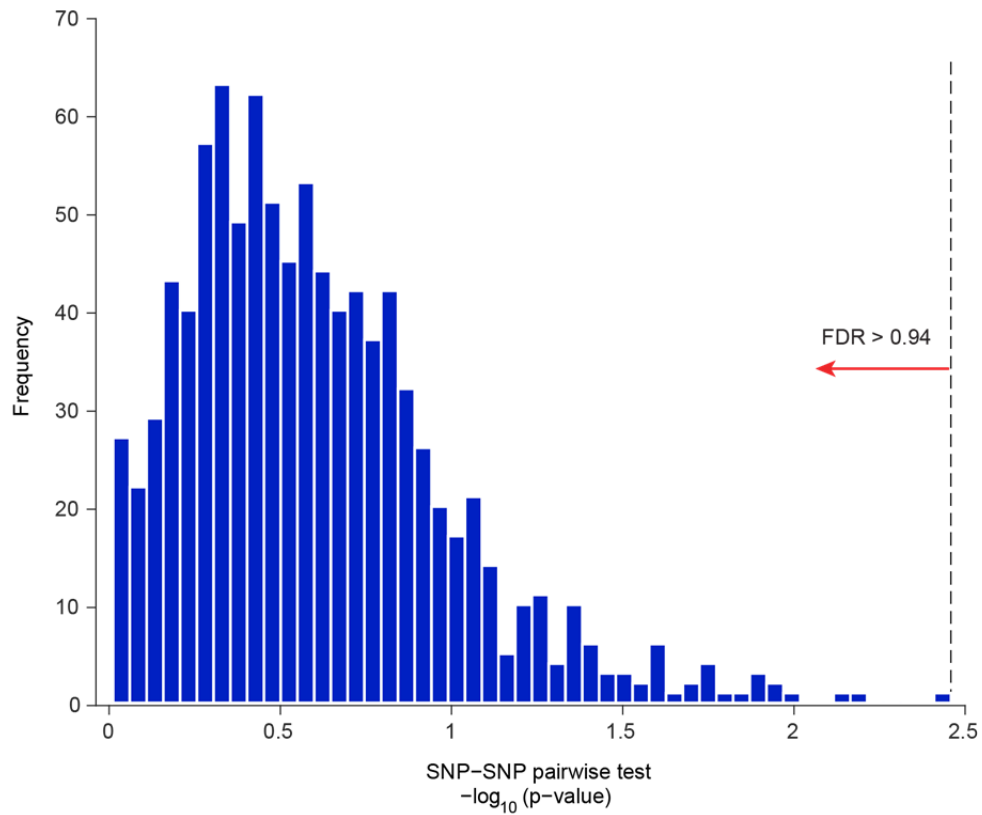
7



8 * Binarization density is determined based on a pilot run (See method)

9 Supplementary Figure 1: Detailed view of the BridGE method for detecting genetic interactions from
10 GWAS data.

11

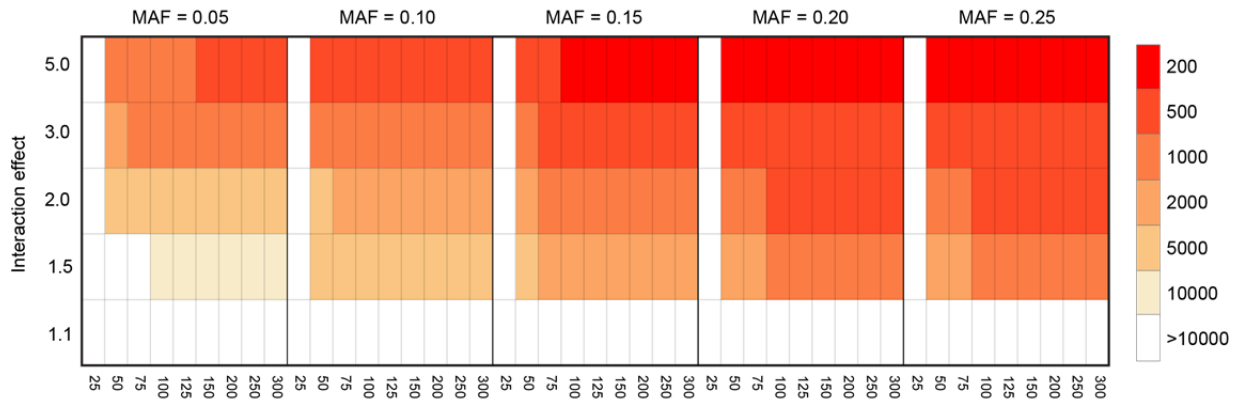


12
 13 Supplementary Figure 2: Distribution of p-values from individual tests for pairwise SNP-SNP interactions
 14 for discovered Parkinson's disease BPM. SNP pairs supporting the pathway-pathway interaction between
 15 the Golgi associated vesicle biogenesis gene set (Reactome) and Fc epsilon receptor I signaling pathway
 16 (KEGG) discovered from the PD-NIA Parkinson's disease cohort were evaluated for association with PD
 17 based on a recessive and dominant disease model. The distribution of maximum $-\log_{10}$ hypergeometric
 18 test p-value of the two models for each SNP pair is plotted. None of the SNP pairs are significant after
 19 multiple hypothesis correction (dashed line at the most significant SNP-SNP pair corresponds to
 20 FDR=0.94).

21

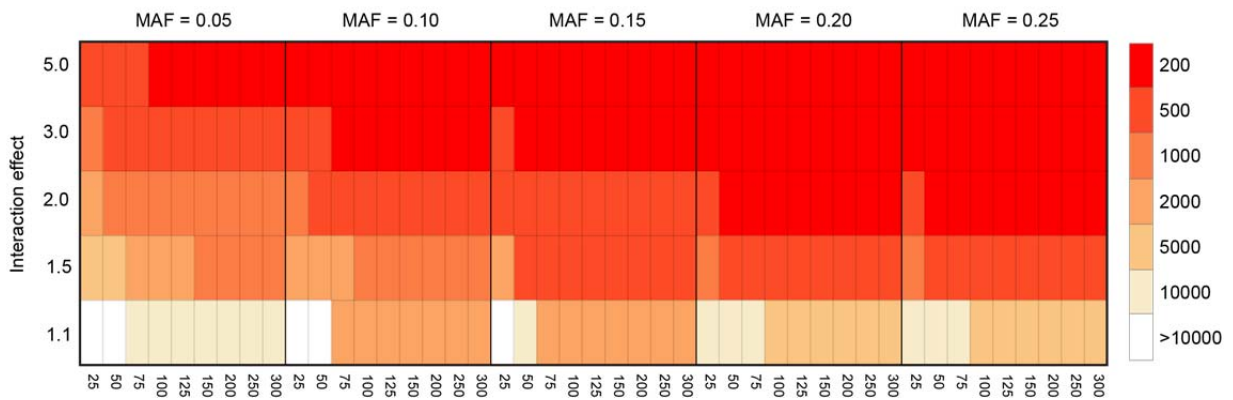
A

FDR = 0.25, Scale = 0.025



B

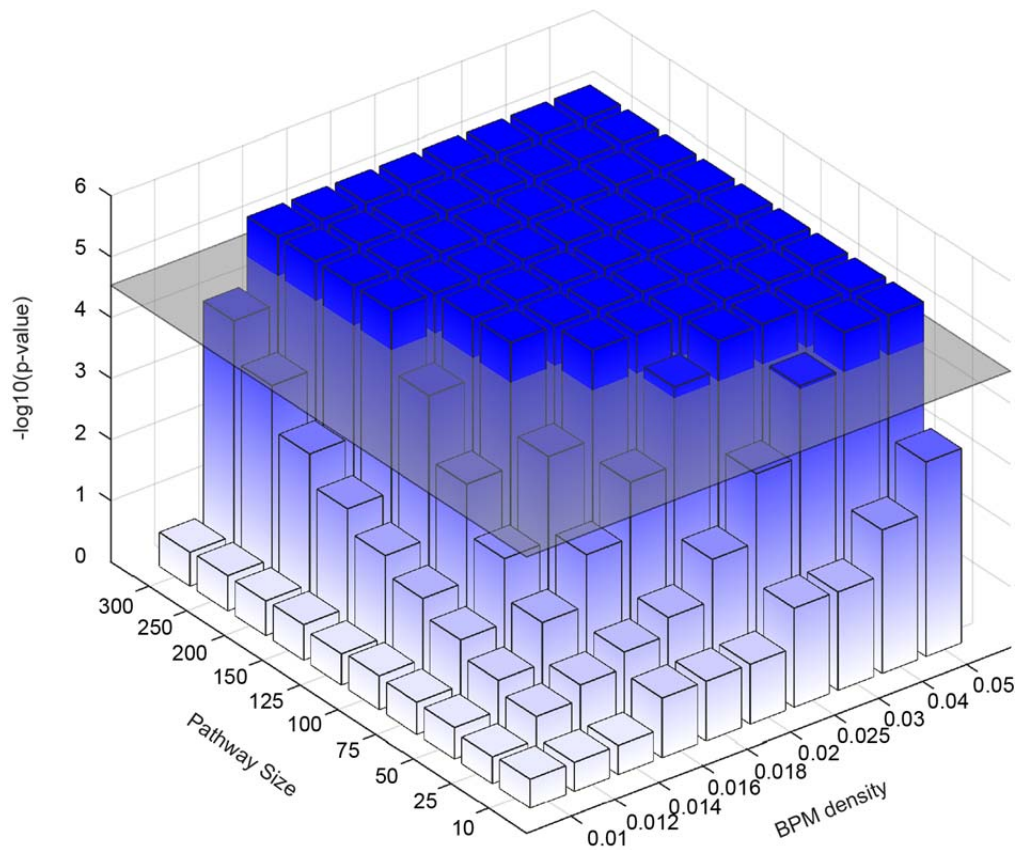
FDR = 0.25, Scale = 0.1



22

23 Supplementary Figure 3: Power analysis of the effect of minor allele frequency (MAF), BPM size,
 24 interaction effect size, and sample size on the discovery of between-pathway interactions. The plot is
 25 same as Fig. 6, but the biological densities used are 2.5% (a) and 10% (b).

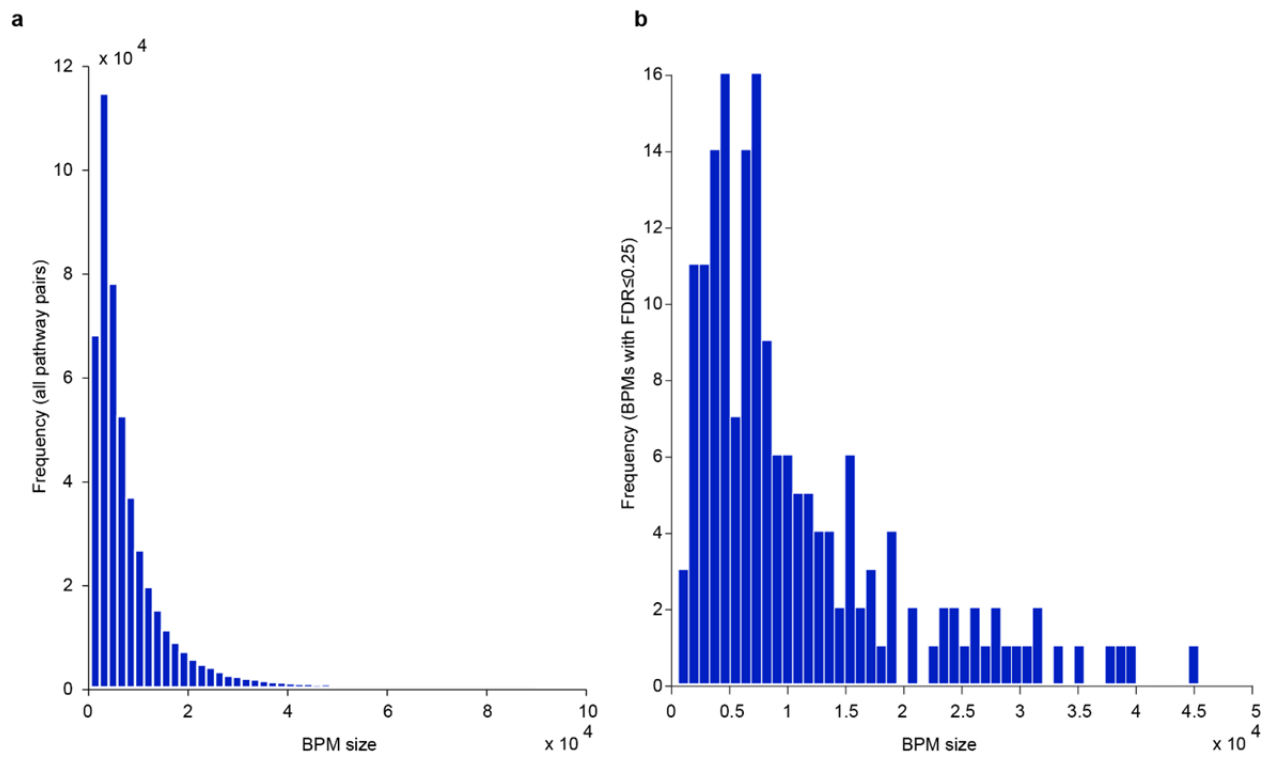
26



27

28 Supplementary Figure 4: Power simulation of the effect of pathway size and interaction density on the
 29 discovery of between-pathway interactions. The BPM significance ($-\log_{10}$ p-value derived from 150,000
 30 SNP permutations) is plotted for 100 embedded BPMs of different sizes and SNP-SNP interaction
 31 densities (online method). The gray plane indicates the p-value cutoff corresponding to the average SNP
 32 permutation p-values ($p = 3.0 \times 10^{-5}$) of the significant BPM discoveries across all GWAS cohorts
 33 ($\text{FDR} \leq 0.25$). Bars exceeding this plane represent BPMs that would have been discovered in this cohort
 34 and provide an estimate of sensitivity of the approach.

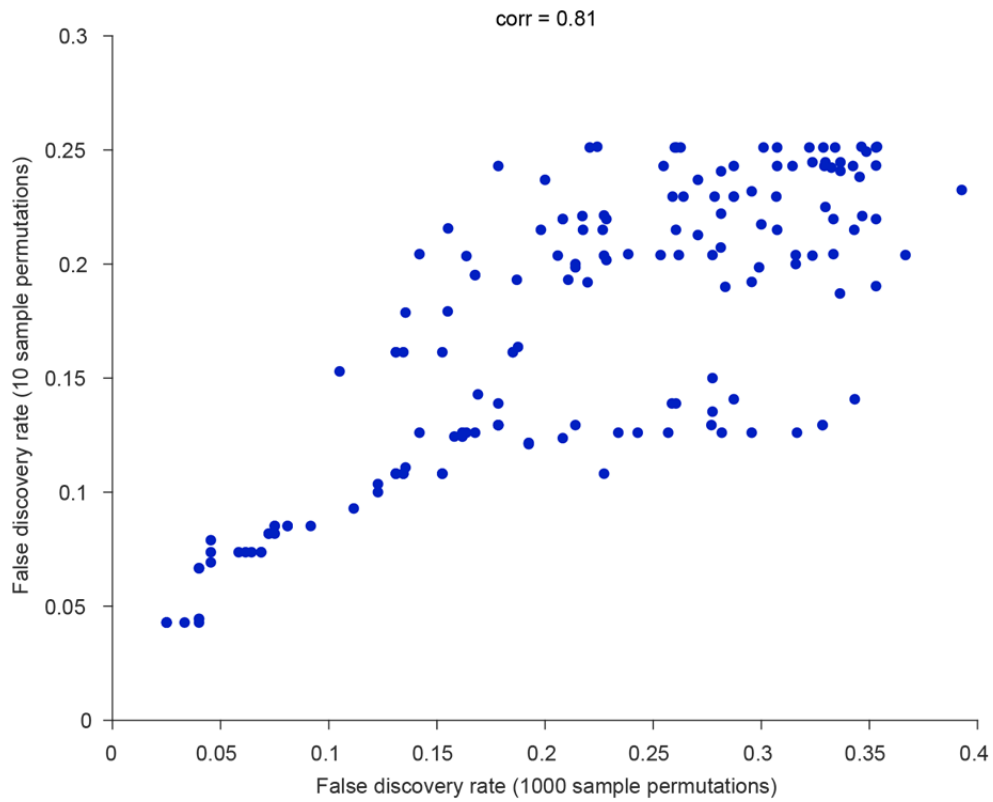
35



36

37 Supplementary Figure 5: Distribution of sizes for discovered BPMs. The size of each candidate BPM was
 38 measured as the total number of possible SNP-SNP pairs between the two pathways. The distribution of
 39 sizes of all possible pathway-pathway pairs is plotted in (a) and only significant BPMs ($FDR \leq 0.25$) from
 40 the PD-NIA cohort are plotted in (b). BPMs discovered by BridGE span a large range of sizes.

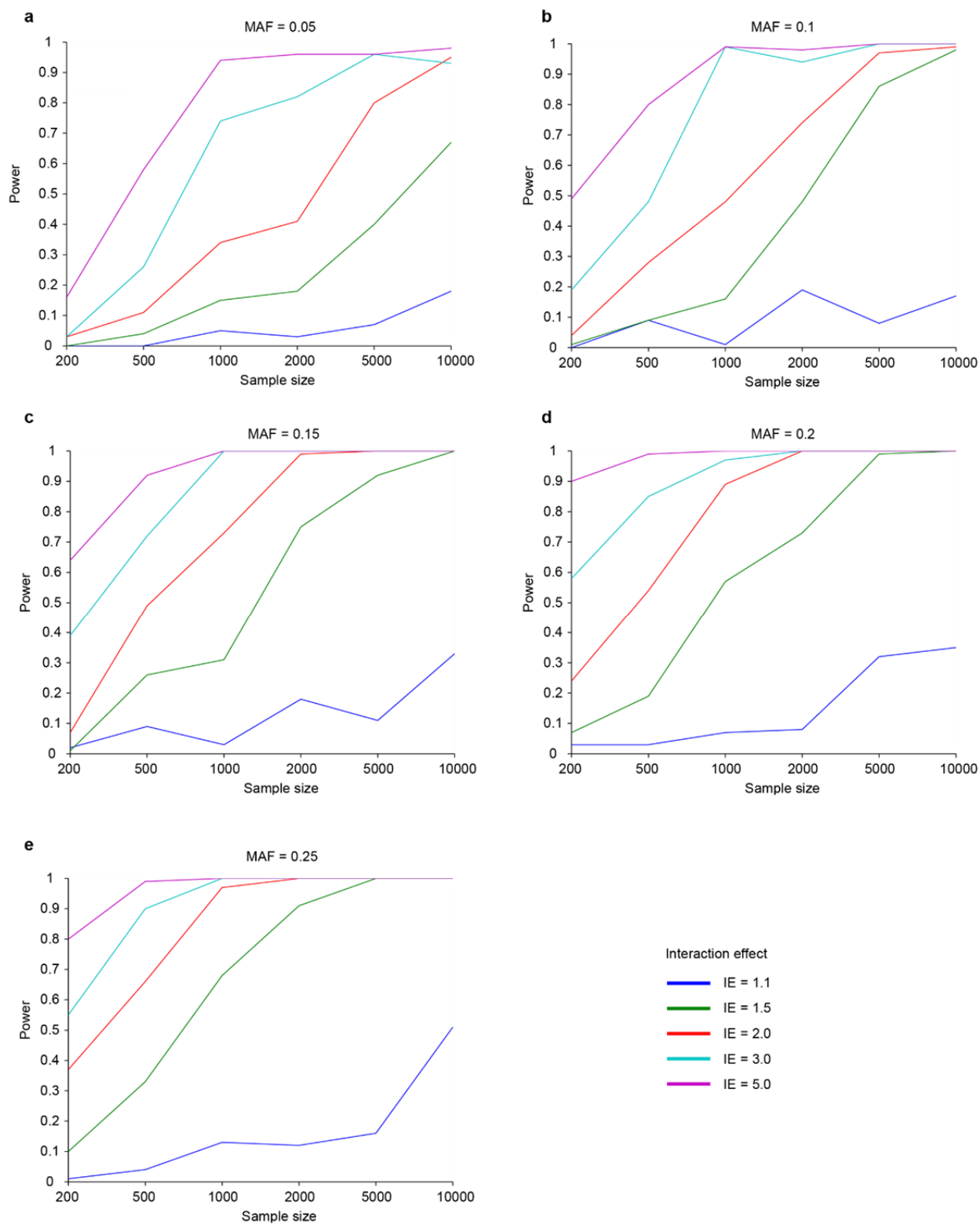
41



42

43 Supplementary Figure 6: Comparison of false discovery rates derived from 10 sample permutations vs.
44 1000 sample permutations using PD-NIA dataset. BPMs that are significant ($FDR \leq 0.25$) based on either
45 10 sample permutations or 1000 permutations were plotted to show the agreement between two
46 permutations.

47



48

49 Supplementary Figure 7: Power simulation of the effect of sample size, interaction effect size (IE) and
 50 minor allele frequency on the discovery of SNP-SNP interactions. The discovery rates of 100 embedded
 51 SNP-SNP interactions in the synthetic datasets with different sample sizes were plotted and colored with
 52 corresponding interaction effect size. Each subplot is corresponded to a different minor allele frequency
 53 assumption: (a) MAF=0.05, (b) MAF=0.1, (c) MAF=0.15, (d) MAF=0.2, (e) MAF=0.25.

54 **Supplementary Discussion**

55 **BridGE results on hypertension and type2 diabetes**

56 Although we did not conduct replication analyses for hypertension or type 2 diabetes, we found that many
57 of the pathways involved in interactions from the discovery cohorts were also highly relevant to the
58 corresponding disease. For example, in the hypertension cohort, we identified a risk-associated BPM
59 interaction involving hypoxia inducible factor (HIF) signaling, whose aberrant expression has been
60 previously associated with hypertension¹. Two BPMs and one WPM, all associated with increased risk,
61 involved the Rho cell motility signaling pathway, which has been previously implicated in the
62 pathogenesis of hypertension². For type 2 diabetes, we discovered BPMs associated with protective
63 effects involving an autoimmune thyroid disease gene set, glycosaminoglycan biosynthesis, and the
64 mTOR signaling pathway, all of which have strong links to diabetes^{3,4,5}.

65

66

67 **Additional Acknowledgements**

68 The genome-wide association datasets (PD-NIA, PD-NGRC, SZ-GAIN, BC-CGEMS-EUR, BC-MCS-
69 JPN, BC-MCS-LTN, HT-eMERGE, ProC-CGEMS, ProC-BPC3 and PanC-PanScan) used in this study
70 were obtained from <https://www.ncbi.nlm.nih.gov/gap> through dbGaP accession numbers:
71 phs000089.v3.p2, phs000196.v3.p1, phs000021.v3.p2, phs000147.v3.p1, phs000517.v3.p1,
72 phs000297.v1.p1, phs000207.v1.p1, phs000812.v1.p1, and phs000206.v5.p3. We acknowledge the
73 Contributing Investigators who submitted data from their original study to dbGaP, the primary funding
74 organization that supported the Contributing Investigators, and the NIH data repository.

75 The genome-wide association datasets (SZ-GAIN, HT-WTCCC, T2D-WTCCC) used in this study
76 were provided by Wellcome Trust Case Control Consortium through Dataset Accession numbers:
77 EGAD00000000006, EGAD00000000009 and EGAD00000000001 and EGAD00000000002. These
78 were funded by the Wellcome Trust under award 076113 and a full list of the investigators who
79 contributed to the generation of the data is available from www.wtccc.org.uk.

80 **PD-NIA (phs000089.v3.p2):**

81 The genotyping of samples was provided by the National Institute of Neurological Disorders and Stroke
82 (NINDS). The dataset used for the analyses described in this manuscript were obtained from the NINDS
83 Database found at <https://www.ncbi.nlm.nih.gov/gap>

84 **PD-NGRC (phs000196.v3.p1):**

85 This work utilized in part data from the NINDS DbGaP database from the CIDR:NGRC PARKINSON'S
86 DISEASE STUDY.

87 **SZ-GAIN (phs000021.v3.p2):**

88 Funding support for the Genome-Wide Association of Schizophrenia Study was provided by the National
89 Institute of Mental Health (R01 MH67257, R01 MH59588, R01 MH59571, R01 MH59565, R01
90 MH59587, R01 MH60870, R01 MH59566, R01 MH59586, R01 MH61675, R01 MH60879, R01
91 MH81800, U01 MH46276, U01 MH46289 U01 MH46318, U01 MH79469, and U01 MH79470) and the
92 genotyping of samples was provided through the Genetic Association Information Network (GAIN). The
93 datasets used for the analyses described in this manuscript were obtained from the database of Genotypes

94 and Phenotypes (dbGaP) found at <http://www.ncbi.nlm.nih.gov/gap> through dbGaP accession number
95 phs000021.v3.p2. Samples and associated phenotype data for the Genome-Wide Association of
96 Schizophrenia Study were provided by the Molecular Genetics of Schizophrenia Collaboration (PI: Pablo
97 V. Gejman, Evanston Northwestern Healthcare (ENH) and Northwestern University, Evanston, IL, USA).

98 **BC-CGEMS-EUR (phs000147.v3.p1):**

99 This dataset was from the Cancer Genetic Markers of Susceptibility (CGEMS) Breast Cancer Genome-
100 wide Association Study with dbGaP accession number phs000147.v3.p1.

101 **BC-MCS-LTN, BC-MCS-JPN (phs000517.v3.p1):**

102 The Multiethnic Cohort and the genotyping in this study were funded by grants from the National
103 Institute of Health (CA63464, CA54281, CA098758, CA132839 and HG005922) and the Department of
104 Defense Breast Cancer Research Program (W81XWH-08-1-0383).

105 **HT-eMERGE (phs000297.v1.p1):**

106 Group Health Cooperative/University of Washington – Funding support for Alzheimer's Disease Patient
107 Registry (ADPR) and Adult Changes in Thought (ACT) study was provided by a U01 from the National
108 Institute on Aging (Eric B. Larson, PI, U01AG006781). A gift from the 3M Corporation was used to
109 expand the ACT cohort. DNA aliquots sufficient for GWAS from ADPR Probable AD cases, who had
110 been enrolled in Genetic Differences in Alzheimer's Cases and Controls (Walter Kukull, PI, R01
111 AG007584) and obtained under that grant, were made available to eMERGE without charge. Funding
112 support for genotyping, which was performed at Johns Hopkins University, was provided by the NIH
113 (U01HG004438). Genome-wide association analyses were supported through a Cooperative Agreement
114 from the National Human Genome Research Institute, U01HG004610 (Eric B. Larson, PI).

115 Mayo Clinic – Samples and associated genotype and phenotype data used in this study were provided
116 by the Mayo Clinic. Funding support for the Mayo Clinic was provided through a cooperative agreement
117 with the National Human Genome Research Institute (NHGRI), Grant #: U01HG004599; and by grant
118 HL75794 from the National Heart Lung and Blood Institute (NHLBI). Funding support for genotyping,
119 which was performed at The Broad Institute, was provided by the NIH (U01HG004424).

120 Marshfield Clinic Research Foundation – Funding support for the Personalized Medicine Research
121 Project (PMRP) was provided through a cooperative agreement (U01HG004608) with the National
122 Human Genome Research Institute (NHGRI), with additional funding from the National Institute for
123 General Medical Sciences (NIGMS) The samples used for PMRP analyses were obtained with funding
124 from Marshfield Clinic, Health Resources Service Administration Office of Rural Health Policy grant
125 number D1A RH00025, and Wisconsin Department of Commerce Technology Development Fund
126 contract number TDF FYO10718. Funding support for genotyping, which was performed at Johns
127 Hopkins University, was provided by the NIH (U01HG004438).

128 Northwestern University – Samples and data used in this study were provided by the NUGene Project
129 (www.nugene.org). Funding support for the NUGene Project was provided by the Northwestern
130 University’s Center for Genetic Medicine, Northwestern University, and Northwestern Memorial Hospital.
131 Assistance with phenotype harmonization was provided by the eMERGE Coordinating Center (Grant
132 number U01HG04603). This study was funded through the NIH, NHGRI eMERGE Network
133 (U01HG004609). Funding support for genotyping, which was performed at The Broad Institute, was
134 provided by the NIH (U01HG004424).

135 Vanderbilt University - Funding support for the Vanderbilt Genome-Electronic Records (VGER)
136 project was provided through a cooperative agreement (U01HG004603) with the National Human
137 Genome Research Institute (NHGRI) with additional funding from the National Institute of General
138 Medical Sciences (NIGMS). The dataset and samples used for the VGER analyses were obtained from
139 Vanderbilt University Medical Center's BioVU, which is supported by institutional funding and by the
140 Vanderbilt CTSA grant UL1RR024975 from NCR/NIH. Funding support for genotyping, which was
141 performed at The Broad Institute, was provided by the NIH (U01HG004424).

142 Assistance with phenotype harmonization and genotype data cleaning was provided by the eMERGE
143 Administrative Coordinating Center (U01HG004603) and the National Center for Biotechnology
144 Information (NCBI). The datasets used for the analyses described in this manuscript were obtained from
145 dbGaP at <http://www.ncbi.nlm.nih.gov/gap> through dbGaP accession number phs000297.v1.p1.

146 **ProC-CGEMS (phs000207.v1.p1):**

147 This data was from the Cancer Genetic Markers of Susceptibility (CGEMS) Prostate Cancer Genome-
148 Wide Association Study.

149 **ProC-BPC3 (phs000812.v1.p1):**

150 The Breast and Prostate Cancer Cohort Consortium (BPC3) genome-wide association studies of advanced
151 prostate cancer and estrogen-receptor negative breast cancer was supported by the National Cancer
152 Institute under cooperative agreements U01-CA98233, U01-CA98710, U01-CA98216, and U01-
153 CA98758 and the Intramural Research Program of the National Cancer Institute, Division of Cancer
154 Epidemiology and Genetics.

155 **PanC-PanScan (phs000206.v5.p3):**

156 This project was funded in whole or in part with federal funds from the National Cancer Institute (NCI),
157 US National Institutes of Health (NIH) under contract number HHSN261200800001E. Additional support
158 was received from NIH/NCI K07 CA140790, the American Society of Clinical Oncology Conquer
159 Cancer Foundation, the Howard Hughes Medical Institute, the Lustgarten Foundation, the Robert T. and
160 Judith B. Hale Fund for Pancreatic Cancer Research and Promises for Purple. A full list of
161 acknowledgments for each participating study is provided in the Supplementary Note of the manuscript
162 with PubMed ID: 25086665.

163

164 **Supplementary References**

165

166 1. Farha S, *et al.* Hypoxia-inducible factors in human pulmonary arterial hypertension: a link to the intrinsic
167 myeloid abnormalities. *Blood* **117**, 3485-3493, <https://doi.org/10.1182/blood-2010-09-306357>, (2011).

168

169 2. Loirand G, Pacaud P. The role of Rho protein signaling in hypertension. *Nat Rev Cardiol* **7**, 637-647,
170 <https://doi.org/10.1038/nrcardio.2010.136>, (2010).

171

172 3. Wang C. The Relationship between Type 2 Diabetes Mellitus and Related Thyroid Diseases. *J Diabetes*
173 *Res* **2013**, 390534, <https://doi.org/10.1155/2013/390534>, (2013).

174

175 4. Gowd V, Gurukar A, Chilkunda ND. Glycosaminoglycan remodeling during diabetes and the role of
176 dietary factors in their modulation. *World J Diabetes* **7**, 67-73, <https://doi.org/10.4239/wjd.v7.i4.67>, (2016).

177

178 5. Verges B, Cariou B. mTOR inhibitors and diabetes. *Diabetes Res Clin Pract* **110**, 101-108,
179 <https://doi.org/10.1016/j.diabres.2015.09.014>, (2015).

180

181